Reliability Oriented OTFS-based LEO Satellites Joint Transmission Scheme

Màrius Caus*, Musbah Shaat*, Ana I. Pérez-Neira*†, Malte Schellmann§, Hanwen Cao§
*Centre Tecnològic de Telecomunicacions de Catalunya (CTTC/CERCA), Castelldefels, Barcelona, Spain
†Department of Signal Theory and Communications, Universitat Politècnica de Catalunya (UPC), Barcelona, Spain
§ Huawei Technologies German Research Center, Munich, Germany

***Abstract*—This paper investigates a dual satellite transmission scheme with coherent reception. The receiver has a single synchronization circuit and is locked to only one of the satellites. Beam-centric pre-compensation techniques are considered in the paper. The cooperation area in which coherent reception is feasible is characterized analytically. The application of precoding to the orthogonal time and frequency space (OTFS) waveform is considered to counteract the residual offsets, which result from the displacement of the receiver from the selected reference point. Numerical evaluations show that the dual satellite scheme improves the system spectral efficiency as well the link reliability in comparison with the single satellite transmission scheme.**

I. Introduction

It is envisioned that in low Earth orbit (LEO) ultra-dense constellations, multiple satellites could be in the field of view (FoV) of users. This opens the door to operate the visible satellites in a coordinated fashion. To unleash the full potential of joint transmission of multiple satellites, the received signals need to be combined coherently, which entails achieving a synchronized reception in time, frequency and phase. Unfortunately, the joint transmission coordinated multi-point (JT-CoMP) schemes specified in latest 3GPP releases [1], are not directly applicable to LEO constellations. The key impediment is that the satellites are continuously moving, which imposes varying propagation delays.

Recent works have proposed distributed precoding algorithms to exploit the macro-diversity offered by LEO satellites, e.g. [2]–[4]. These schemes assume that signals that come from different satellites are synchronously received. In this work we have examined with more thoroughness the time and the frequency misalignment that result from the inter-satellite distance. To reduce the differential delay and the frequency shift that is observed by the user equipment (UE), beam-centric pre-compensation techniques have been adopted. That is, transmission parameters are adjusted so that any UE located at the selected reference point is able to receive satellite signals perfectly synchronized. The time and frequency offsets are bound to arise if the UE is located away from the reference point. To counteract the residual offsets, we propose to adopt the recently proposed orthogonal time and frequency space (OTFS) waveform [5]. Several works have investigated the application of OTFS over satellite links, e.g., [6], [7]. In the same vein, we have developed a dual satellite transmission scheme that achieves coherent signal reception. The improvement with respect to previous OTFS works is that it supports cooperative transmission in LEO constellations. The most remarkable feature of the new transmission strategy stems from the fact that the receiver only needs to be locked to one satellite. The innovation relies on precoding the symbols of the furthest satellite to compensate differential delays and frequency shifts with respect to the closest satellite. To generate the precoder, the UE is only required to report its position to the network. Hence, in low-mobility scenarios, it is unlikely that the system is affected by feedback delay issues. The merits of OTFS are also based on the possibility of transmitting a single cyclic prefix (CP) block per frame. Numerical results reveal that dual satellite transmission achieve significant gains in terms of spectral efficiency and reliability compared to the single satellite service.

II. Targeted scenario and cooperation area

In the scenario under study, several satellites are able to adjust the transmission parameters to attain synchronization at a given location within the beam coverage, which is referred to as the reference point. If the UE is not near the reference spot, differential delays between satellite signals will arise. To determine the maximum displacement that is tolerated with respect to the reference point, it is essential to know the maximum tolerable misalignment. For instance, in orthogonal frequency division multiplexing (OFDM)-like waveforms, the time offset is not an issue if all signals are received within the CP block. In such a case, the region where the path delays do not exceed the CP is referred to as the cooperation area.

To find the boundaries of the cooperation area when OFDM-like signals are adopted in the satellite interface, we first represent the position of the satellites and the reference point as shown in Figure 1. The spherical coordinates of the k-th satellite can be represented by $(R_E + h, \alpha_k, \lambda_k)$, where R_E is the radius of the Earth, h is the altitude of the orbit and α_k, and λ_k are the geocentric latitude and longitude, respectively. The coordinates of the reference point are given by $(R_E, \alpha_0, \lambda_0)$. The position of the *k*-th satellite can also be represented by the distance $r_{k,0}$, the azimuth $\phi_{k,0}$, and the elevation $\theta_{k,0}$, which are measured with respect to the local tangent plane (LTP) with its origin at the reference point. For notational convenience, the first satellite (to be referred to as satellite#1) is assumed to be closer to the reference point than the second satellite (to be referred to as satellite#2). From Figure 1, it can be inferred that the differential propagation delay at the reference point can be computed as $\Delta_{t,0} = \frac{1}{c}|r_{1,0} - r_{2,0}|$, where c is the speed of light. Note that timing advance for one of the satellites is utilized to enable time-synchronous reception of both signals in the reference point.

 DOI 10.1109/GCWkshps56602.2022.10008593

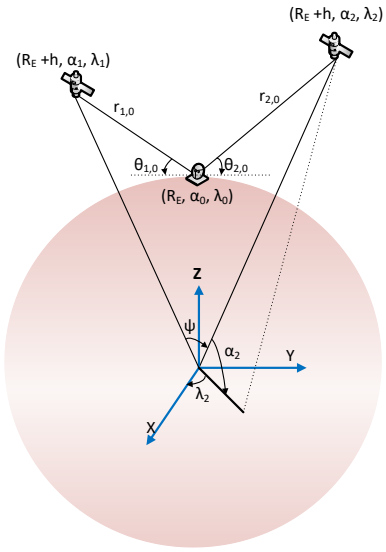

Fig. 1. Reference scenario in dual satellite transmission systems.

Without loss of generality, we consider that the coordinates of the target UE are given by $(R_E, \alpha_p, \lambda_p)$. The slant range between the UE and the k-th satellite can be readily computed from the Cartesian coordinates in this form

$$r_{k,p} = \|R_E\,(\cos\alpha_p\cos\lambda_p, \cos\alpha_p\sin\lambda_p, \sin\alpha_p) - (R_E+h)\,(\cos\alpha_k\cos\lambda_k, \cos\alpha_k\sin\lambda_k, \sin\alpha_k)\|\,. \quad (1)$$

We declare that the UE is within the cooperation area if

$$|r_{1,p} \pm c\Delta_{t,0} - r_{2,p}| \leq cT_{\text{CP}}, \quad (2)$$

where T_{CP} denotes the duration of the CP. If satellite#1 is closer to the UE than satellite#2, then $\Delta_{t,0}$ is positive, meaning that satellite#2 must advance its transmission. Otherwise, if $\Delta_{t,0}$ is negative, the timing need to be adjusted by satellite#1. Suppose that the UE is separated by d meters from the reference point and rotated by Δ_ϕ. By applying the spherical law of cosines to the spherical triangle represented in Figure 2, we can readily express α_p and λ_p as function of d, Δ_ϕ, α_0 and λ_0. For the sake of brevity, the expressions are not provided. It can be verified that the maximum distance d that a given UE can move away from the reference point without leaving the cooperation area, which is referred to as d_{MAX}, is achieved when (2) is satisfied with equality. The value of d_{MAX} for a given Δ_ϕ and T_{CP} can be computed via numerical calculations. Therefore, the exact shape of the cooperation area can be determined if the positions of the satellites are known.

III. System Model

In this section, the reference scenario is introduced. We have considered that the UE is able to simultaneously establish two directional links with two LEO satellites that are in the FoV. The UE is located within a beam of radius R_B. The satellites are able to adjust the time and the frequency as described in Section II. Without loss of generality, it is assumed that satellite#1 is located in the closest position to the reference point. To represent the position of the k-th satellite relative to the user's location, we use the spherical coordinates (r_k, θ_k, ϕ_k).

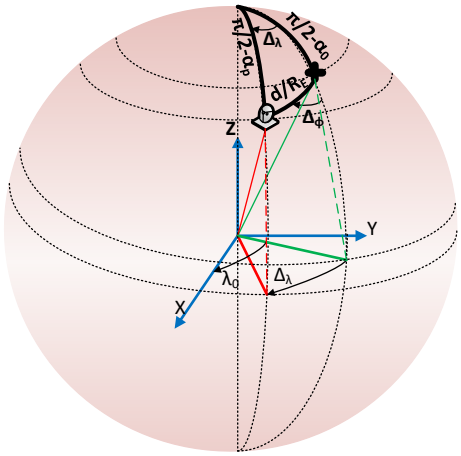

Fig. 2. Representation of the spherical triangle used to compute α_p,λ_p.

In the proposed scheme, the transmission bandwidth B_W is partitioned into M subcarriers that are spaced Δ_f apart in frequency. The transmitted signal frame is formed by L multicarrier symbols. At each subcarrier, symbols are transmitted with a rate $1/T$, where T is the symbol period. The system under study is designed so that $T \cdot \Delta_f = 1$, which leads to a sampling period that is given by $T_s = T/M$. We stick to the case where the propagation channel is dominated by the line-of-sight (LoS) component. Therefore, the detrimental effects induced by the environment only include the delay τ and the Doppler shift ϵ. The satellites compensate for both, the Doppler shift and the delay at the selected reference point location. The time and the frequency offset associated to the k-th satellite link can be formulated at the reference point as

$$\tau_{k,0} = \frac{r_{k,0}}{c} = \frac{i_{k,0}}{M\Delta_f} = i_{k,0}\frac{T}{M} \quad (3)$$

$$\epsilon_{k,0} = \frac{q_{k,0}+\kappa_{k,0}}{LT} = (q_{k,0}+\kappa_{k,0})\frac{\Delta_f}{L}, \quad (4)$$

where $i_{k,0}$ and $q_{k,0}$ are integers. The term $-1/2 \leq \kappa_{k,0} \leq 1/2$ denotes the fractional Doppler shift from the nearest grid point. This paper targets enhancing the communication reliability. Hence, both satellites transmit the same information. In such a case, the discrete-time domain signal transmitted by the k-th satellite is expressed as

$$s_k[n] = \sqrt{P_T}e^{-j\frac{2\pi(q_{k,0}+\kappa_{k,0})}{ML}n}s[n], \quad (5)$$

where $\sqrt{P_T}$ is the transmit power and $s[n]$ is the modulated signal. The satellite signals lie within the category of single-antenna transmission as each beam is driven by a single feed.

To distinguish between the different satellites, the UE is equipped with a uniform planar array (UPA) of dimension $N_x \times N_y$. Thus, the total number of antenna elements is $N_R = N_x N_y$. To define the system model, we assume that the satellite#2 advances its transmission by $\Delta_{t,0}$ seconds (or equivalently by $i_{2,0} - i_{1,0}$ samples). If we stack the output of each antenna in column-wise manner, the received signal becomes

$$\begin{aligned}\mathbf{y}[n] = \;& \mathbf{h}_1 e^{j\frac{2\pi}{ML}(q_1+\kappa_1)(n-i_1)}s_1[n-i_1] + \mathbf{w}[n] + \\ & \mathbf{h}_2 e^{j\frac{2\pi}{ML}(q_2+\kappa_2)(n-i_2)}s_2[n-i_2+i_{2,0}-i_{1,0}],\end{aligned} \quad (6)$$

where the reception is contaminated by the noise vector $\mathbf{w}[n] \in \mathbb{C}^{N_R \times 1}$. In notational terms, the triplet (i_k, q_k, κ_k) denotes the delay index, the Doppler index and the fractional Doppler shift associated to the k-th satellite. The channel vector can be formulated as

$$\mathbf{h}_k = \sqrt{\frac{G_k G_R(\theta_k, \phi_k)}{L_k K_B B_W T}} e^{-j\frac{2\pi r_k}{\lambda}} \mathbf{a}(\theta_k, \phi_k) \tag{7}$$

$$[\mathbf{a}(\theta_k, \phi_k)]_{n+N_x m} = e^{j\frac{2\pi d_A}{\lambda}(n\cos\theta_k \cos\phi_k + m\cos\theta_k \sin\phi_k)}, \tag{8}$$

for $1 \leq k \leq 2$, $0 \leq n \leq N_x - 1$ and $0 \leq m \leq N_y - 1$. We use $[\mathbf{a}]_i$ to refer to the i-th element of the steering vector $\mathbf{a}$. The entries of $\mathbf{a}$ are formulated as function of antenna spacing d_A, the wavelength λ and the position of the k-th satellite that is located at (θ_k, ϕ_k). The magnitude of the channel depends on the antenna gain of the k-th satellite G_k, the antenna gain of the radiating element $G_R(\theta_k, \phi_k)$, the free space loss L_k, the Boltzmann constant K_B, the bandwidth B_W and the system noise temperature T.

Since the visible satellites convey the same information, the two satellite links are combined at the receiver as follows,

$$z[n] = \mathbf{f}_{\text{BB}}^{\text{H}} \mathbf{F}_{\text{RF}}^{\text{H}} \mathbf{y}[n]. \tag{9}$$

The decoding matrix is formed by $\mathbf{F}_{\text{RF}} \in \mathbb{C}^{N_R \times N_{\text{RF}}}$ and $\mathbf{f}_{\text{BB}} \in \mathbb{C}^{N_{\text{RF}} \times 1}$, which perform the spatial processing in the analog and the digital domain, respectively. We have considered a fully-connected hybrid beamforming architecture to reduce the cost and the hardware complexity, with respect to full-digital architectures [8]. In the next stage, the timing and the frequency are adjusted to attain synchronization with satellite#1. Although the UE establishes two satellite links, it only employs a single synchronization circuit to reduce the complexity. This works because the two satellites are synchronized with respect to the reference point. Upon combining the signals and compensating time and frequency offsets with respect to satellite#1, the received signal can be formulated as $z_1[n] = z[n + i_1] e^{-j\frac{2\pi}{ML}(q_1 + \kappa_1 - q_{1,0} - \kappa_{1,0})n}$. After plugging (5), (6) and (9) into $z_1[n]$, we get

$$\begin{aligned} z_1[n] \quad &= \mathbf{f}_{\text{BB}}^{\text{H}} \mathbf{F}_{\text{RF}}^{\text{H}} \mathbf{w}[n] + \sqrt{P_T} \mathbf{f}_{\text{BB}}^{\text{H}} \mathbf{F}_{\text{RF}}^{\text{H}} (\mathbf{h}_1 s[n] + \\ &\quad \mathbf{h}_2 e^{j\frac{2\pi}{ML}(q_{\text{eff}} + \kappa_{\text{eff}})n} e^{j\delta_\phi} s[n - i_{\text{eff}}]\Big), \end{aligned} \tag{10}$$

where $i_{\text{eff}} = i_2 - i_{2,0} - i_1 + i_{1,0}$. Concerning the frequency offset, we denote respectively q_{eff} and κ_{eff} the integer and the fractional parts of

$$q_2 + \kappa_2 - q_{2,0} - \kappa_{2,0} - (q_1 + \kappa_1 - q_{1,0} - \kappa_{1,0}).$$

The term δ_ϕ represents the phase offset that arises in the signal of satellite#2, after applying time and frequency corrections to synchronize with satellite#1.

Under the premise that the steering vectors are estimated by the UE, the analog beamforming matrix can be designed according to the phased array beamforming, i.e., $\mathbf{F}_{\text{RF}} = \frac{1}{\sqrt{N_R}} [\mathbf{a}(\theta_1, \phi_1) \quad \mathbf{a}(\theta_2, \phi_2)]$. This design complies with the constraint that imposes constant amplitude to all coefficients of $\mathbf{F}_{\text{RF}}$. The case of UE with large number of antennas is considered. Accordingly, the beamforming will be very directional. Furthermore, if the angular separation between satellites is sufficiently high, it can be safely assumed that $\mathbf{a}^{\text{H}}(\theta_1, \phi_1) \mathbf{a}(\theta_2, \phi_2) / N_R \ll 1$. Therefore, inter-satellite-interference will be neglected unless otherwise stated. Under this hypothesis and together with perfect channel state information at the receiver, we can set the weights of the receive vector according to the matched filter, leading to

$$\mathbf{f}_{\text{BB}} = \begin{bmatrix} h_1 & h_2 e^{j\delta_\phi} \end{bmatrix}^{\text{T}}, \tag{11}$$

with $h_i = \sqrt{P_T / N_R} \mathbf{a}^{\text{H}}(\theta_i, \phi_i) \mathbf{h}_i$, for $i = 1, 2$. The received signal can be compactly expressed as

$$z_1[n] = |h_1|^2 s[n] + |h_2|^2 e^{j\frac{2\pi}{ML}(q_{\text{eff}} + \kappa_{\text{eff}})n} s[n - i_{\text{eff}}] + v[n], \tag{12}$$

where $v[n] = \mathbf{f}_{\text{BB}}^{\text{H}} \mathbf{F}_{\text{RF}}^{\text{H}} \mathbf{w}[n]$. Assuming that the steering vectors become asymptotically orthogonal with increasing the number of antennas and further that the noise samples at the input of the receiver are distributed as $\mathbf{w}[n] \sim \mathcal{CN}(\mathbf{0}_{N_R}, \mathbf{I}_{N_R})$, then the filtered noise can be modelled as $v[n] \sim \mathcal{CN}\left(0, |h_1|^2 + |h_2|^2\right)$.

To improve the resilience to doubly selective channels and the efficiency of the OFDM multi-carrier modulation scheme, we propose to adopt the OTFS modulation with the rectangular pulse-shaping waveform [5]. Remarkably, in OTFS, it is possible to transmit a single CP block ahead of the frame instead of every symbol, as in the case of OFDM. Accordingly, the modulated signal is formulated as

$$s[n] = \begin{cases} u[n - L_{\text{CP}}] & L_{\text{CP}} \leq n \leq ML + L_{\text{CP}} - 1 \\ u[n + ML - L_{\text{CP}}] & 0 \leq n \leq L_{\text{CP}} - 1 \end{cases} \tag{13}$$

where,

$$u[n] = \sum_{l=0}^{L-1} \sum_{m=0}^{M-1} X[l, m] g_m[n - lM]. \tag{14}$$

The subcarrier pulses are given by $g_m[n] = \frac{1}{\sqrt{M}} e^{j\frac{2\pi}{M}nm}$, for $0 \leq n \leq M - 1$ and 0 otherwise. In the OTFS scheme, the symbol transmitted in the time-frequency position (l, m) is generated as

$$X[l, m] = \frac{1}{\sqrt{ML}} \sum_{q=0}^{M-1} \sum_{i=0}^{L-1} x[i, q] e^{j2\pi\left(\frac{li}{L} - \frac{mq}{M}\right)}. \tag{15}$$

Notice that the information symbols $\{x[i, q]\}$ are fed into a 2D unitary transform, which is referred to as inverse symplectic finite Fourier transform (ISFFT). It is worth emphasizing that in OTFS, (integer) time and frequency dispersion can be efficiently combated if $|i_{\text{eff}}| < M$ and $|q_{\text{eff}}| < L$.

IV. Joint transmission scheme

In this section, we develop a joint transmission scheme suitable for LEO satellite systems and adapted to the OTFS modulation scheme. The objective is to enhance the received signal-to-noise ratio (SNR) by coherent superposition of the different satellites signals.

By feeding $\{z_1[L_{\text{CP}}], \cdots, z_1[ML + L_{\text{CP}} - 1]\}$ into the OTFS demodulator and performing the block-based processing

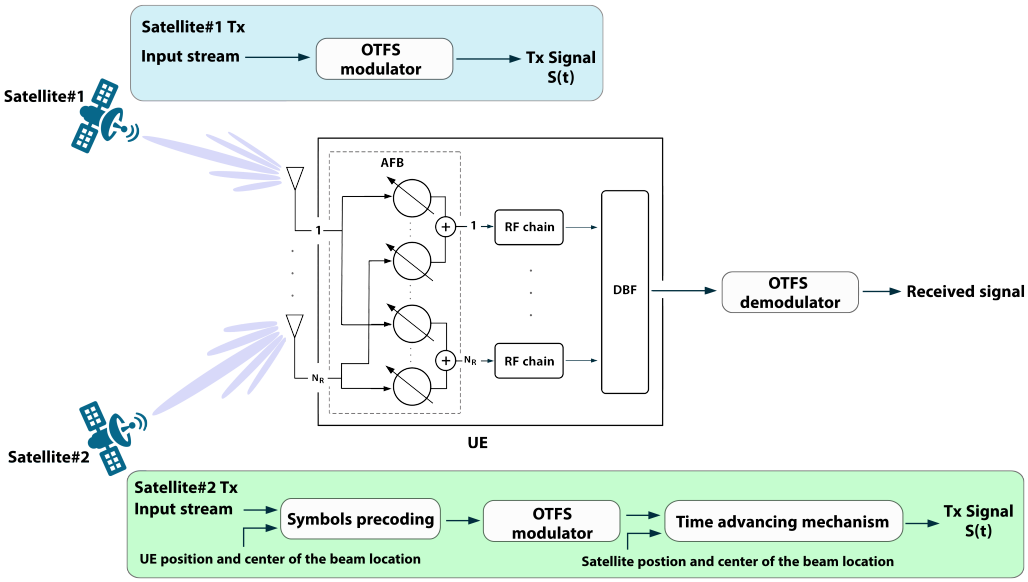

Fig. 3. Block diagram of the proposed two satellites scheme with coherent reception.

proposed in [5], we can compactly express the input-output relation using this matrix notation

$$\hat{\boldsymbol{x}} = \left(|h_1|^2 \boldsymbol{I}_{ML} + |h_2|^2 \boldsymbol{H}_{\text{eff}}\right) \boldsymbol{x} + \boldsymbol{v}, \tag{16}$$

where $\hat{\boldsymbol{x}} \in \mathbb{C}^{ML\times 1}$ is the demodulated symbol vector and $\boldsymbol{v} \in \mathbb{C}^{ML\times 1}$ is the noise vector. Since OTFS employs unitary transforms, the noise vector follows the distribution $\boldsymbol{v} \sim \mathcal{CN}(\mathbf{0}_{ML}, (|h_1|^2 + |h_2|^2)\mathbf{I}_{ML})$. The symbol vector is obtained by stacking column-wise the information symbols as follows,

$$\boldsymbol{x} = [\mathbf{x}_0^{\mathrm{T}}, \cdots, \mathbf{x}_{L-1}^{\mathrm{T}}]^{\mathrm{T}}, \tag{17}$$

where $\mathbf{x}_l = [x[l,0], \cdots, x[l,M-1]]^{\mathrm{T}}$. The effective channel matrix is defined by

$$\mathbf{H}_{\text{eff}} = \sum_{i=-P}^{P} c_i \mathbf{T}^i. \tag{18}$$

The fractional Doppler shift spreads out the power of a symbol over the neighboring symbols. The interference is determined by the Dirichlet kernel functions. Therefore, the coefficient associated to the i-th channel component is given by

$$c_i = \frac{1}{L} e^{j\frac{\pi}{L}(\kappa_{\text{eff}}-i)(L-1)} \frac{\sin\left(\pi(\kappa_{\text{eff}}-i)\right)}{\sin\left(\frac{\pi}{L}(\kappa_{\text{eff}}-i)\right)}. \tag{19}$$

Taking into account the time localization properties of the Dirichlet kernel functions, it is common to assume that the interference comes from a small neighborhood around the symbol of interest. This means that $2P+1 < L$. In this work we consider that most of the energy is confined in the main beam and the four closest adjacent beams, thus $P = 3$. Finally, the entries of the i-th tap are evaluated according to (20), where $0 \le p,t \le ML-1$. The values of n and m in the definition of the (p,t)-th entry of $\mathbf{T}^i$ can be computed as $n = \lfloor p/M \rfloor$ and $m = p - nM$. Due to matrix $\mathbf{H}_{\text{eff}}$, the satellite#2 signal is not added coherently with satellite#1 signal. Thanks to the favourable properties of OTFS, there are only $2P+1$ nonzero elements in each row and column of $\mathbf{H}_{\text{eff}}$. Another remarkable property is that $\mathbf{H}_{\text{eff}}\mathbf{H}_{\text{eff}}^{\mathrm{H}} \approx \mathbf{I}_{ML}$. This result can be inferred from the factorization derived in [5], namely,

$$\mathbf{H}_{\text{eff}} = (\mathbf{F}_L \otimes \mathbf{I}_M)\, \Pi^{i_{\text{eff}}} \boldsymbol{\Delta}^{q_{\text{eff}}+\kappa_{\text{eff}}} \left(\mathbf{F}_L^{\mathrm{H}} \otimes \mathbf{I}_M\right), \tag{21}$$

where $\boldsymbol{\Delta} = \text{diag}\left[1, e^{\frac{j2\pi}{ML}} \cdots e^{\frac{j2\pi(ML-1)}{ML}}\right]$, $\boldsymbol{F}_L \in \mathbb{C}^{L\times L}$ is the DFT matrix and the permutation matrix is given by

$$\Pi = \begin{bmatrix} 0 & \cdots & 0 & 1 \\ 1 & \ddots & 0 & 0 \\ \vdots & \ddots & \ddots & \vdots \\ 0 & \cdots & 1 & 0 \end{bmatrix} \in \mathbb{C}^{ML\times ML}. \tag{22}$$

Clearly the factorization of $\mathbf{H}_{\text{eff}}$ indicates that the conjugate precoding is capable of pre-compensating the time and the frequency offset induced by the differential slant range. The alternative of choosing the location of the UE as the reference point, leads to the same result without precoding. However, the coordinates of the UE must be available at both satellites. In the proposed transmission scheme, only satellite#2 is required to track the UE, which simplifies the implementation. If the UE is provisioned with the satellite ephemeris and knows the location of the reference point, then it follows that the compensation could be done at the receiver before the baseband combining. The technique devised in this section aims to move the complexity from the UE to the network. For this reason we favour the proposed precoding over the rest of solutions. In such a case, if satellite#2 precodes the symbol vector as $\mathbf{H}_{\text{eff}}^{\mathrm{H}}\boldsymbol{x}$, then the input-output relation can be formulated as

$$\hat{\boldsymbol{x}} = \left(|h_1|^2 + |h_2|^2\right) \boldsymbol{x} + \boldsymbol{v} + \boldsymbol{r}. \tag{23}$$

After OTFS demodulation, data symbols can be individually detected. The vector $\boldsymbol{r}$ is the residual interference that originates from compensating for the fractional Doppler with a

$$[\mathbf{T}^i]_{p,t} = \begin{cases} e^{-j\frac{2\pi n}{L}} e^{j\frac{2\pi}{ML}(q_{\text{eff}}+i) \bmod (m-i_{\text{eff}},M)} & \text{if } t = \bmod (m-i_{\text{eff}},M) + M \bmod (n-q_{\text{eff}}-i,L) \text{ and } m < i_{\text{eff}} \\ e^{j\frac{2\pi}{ML}(q_{\text{eff}}+i) \bmod (m-i_{\text{eff}},M)} & \text{if } t = \bmod (m-i_{\text{eff}},M) + M \bmod (n-q_{\text{eff}}-i,L) \text{ and } m \geq i_{\text{eff}} \\ 0 & \text{otherwise,} \end{cases} \quad (20)$$

reduced number of taps, i.e., $2P+1 < L$. The same precoder has been proposed in multi-user massive multiple-input multiple-output systems [9]. To the best of our knowledge this precoding strategy has not been applied to OTFS-based dual satellite systems. In the proposed scenario, the transmitter needs to be aware of the effective channel. One option is to estimate the channel state information (CSI) at the receiver and report it to the transmitter. Alternatively, the channel could be generated at the transmitter under the premises that satellite trajectories are known and that the UE reports its position to the network. With this information, it is possible to determine the differential delay and the differential Doppler shift with respect to the reference point. Then, the closed-form expression of the channel components, i.e., $\{c_i \boldsymbol{T}^i\}$, can be computed. In low-mobility scenarios, where the position of the UE varies on a time scale slower that the round trip time, the UE geographic information can be used in satellite#2 for several transmissions before needed to be updated (either due to UE or satellite#2 mobility). Figure 3 shows the block diagram of the proposed scheme, where also the block diagram of the hybrid analog-digital combiner is depicted. Note that in the transmission chain of satellite#1, the location of the UE is not required, but only the coordinates of the reference point.

A. Comparison between OTFS and OFDM

This section highlights the limitations of OFDM in dual satellite transmissions schemes as well as the suitability of OTFS. In this respect, the key limiting factor is the overhead. While OTFS transmits a CP of L_{CP} samples every L multicarrier symbols, OFDM transmits the same redundancy ahead of each multicarrier symbol. Therefore, the efficiency loss factor in OTFS and OFDM becomes $\eta_{\text{OTFS}} = \frac{ML}{ML+L_{\text{CP}}}$ and $\eta_{\text{OFDM}} = \frac{M}{M+L_{\text{CP}}}$, respectively. From these definitions we can observe that the spectral and the energy efficiency losses are more significant in OFDM than in OTFS. The overhead could be reduced in OFDM by transmitting shorter CP blocks. However, this would have an impact on the size of the cooperation area.

V. Numerical results

In this section, the proposed transmission scheme is compared against an OFDM-based system, where the information is only received from the closest satellite. The techniques that are assessed are referred to as OTFS dual and OFDM single.

To construct the constellation, we have used the Walker's method. The orbital characteristics are obtained from the Starlink LEO constellation network described in [10]. More precisely, the number of orbital planes is 72, the number of satellites per plane is 22, the altitude of the orbit is $h = 550$ Km and the orbital inclination is 53°. The system parameters are listed in Table I. The effective isotropic radiated power (EIRP), the system temperature and the frequency are reported in [11]. The large subcarrier spacing is selected to achieve high robustness to the Doppler effects. Based on the subcarrier spacing, the number of carriers is chosen to approximately occupy a bandwidth of 250 MHz. The number of multicarrier symbols that forms the frame is set to $L = 32$. When dual satellite transmission is adopted, we set $L_{\text{CP}} = M - 1$. For single satellite transmission, the normal CP specified in [12] is used, which corresponds to $L_{\text{CP}} = 72$.

TABLE I
System parameters

System Parameters	Value
Frequency	$f_c = 13.5$ GHz
Size of the frame	$M = 1024$, $L = 128$
Sampling period	$T_s = \frac{T}{M} = 4.069$ ns
Subcarrier spacing	$\Delta_f = 240$ KHz
Bandwidth	$B_w = M\ \Delta_f = 245.76$ MHz
EIRP	$P_T + G_T = 67.7$ dBm
System temperature	$T = 290$ K
Antenna element gain	$G_R = 0$ dB

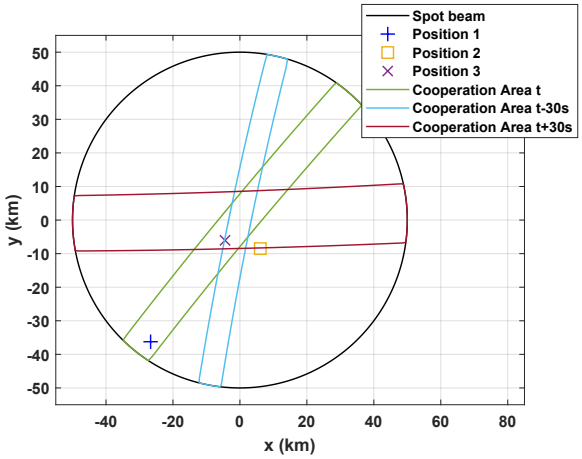

Fig. 4. Representation of the cooperation area.

To perform link level simulations, we have taken a snapshot of the satellite constellation. We assume that the satellites deploy Earth-fixed beams of radius 50 Km. The center of the target beam is located in Munich. At this location, it is highly likely that any UE within the beam could see at least two satellites in the FoV. In the time instant of interest, which is referred to as t, the position of the two closest satellites (if the center of the beam is taken as a reference point) are given by $(r_{1,0}, \theta_{1,0}, \phi_{1,0}) = (588.08\text{Km}, 68.35°, 359.91°)$ and $(r_{2,0}, \theta_{2,0}, \phi_{2,0}) = (657.97\text{Km}, 55.12°, 349.19°)$. It can be inferred that the differential delay is $\Delta_t = 0.233$ ms. If the satellite#2 applies the time-advance mechanism, the analytical studies conducted in Section II reveal that there exists a cooperation area where the two satellite signals arrive at the receiver within the CP. The two-dimensional plot of the resulting cooperation area is represented in Figure 4. We select three different positions. An interesting conclusion that

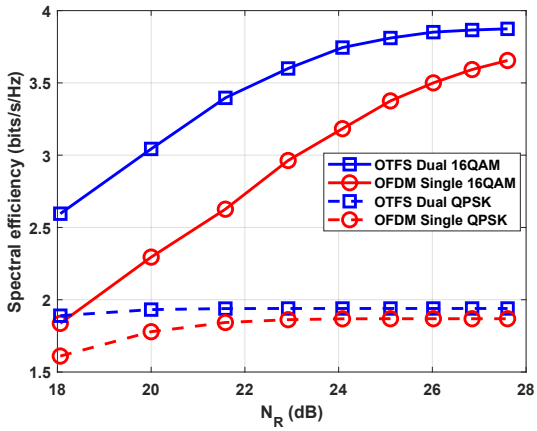

Fig. 5. Spectral efficiency vs. the number of receiving antennas.

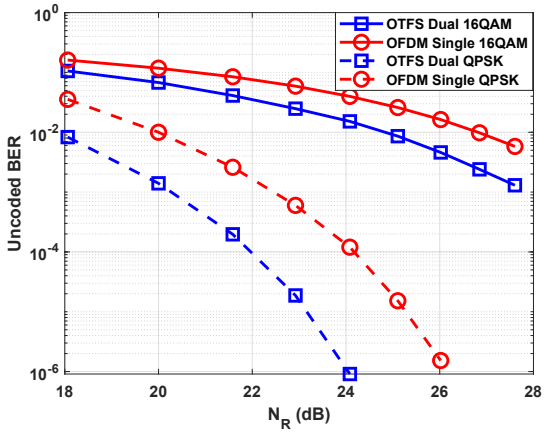

Fig. 6. Uncoded BER vs. the number of receiving antennas.

can be inferred from Figure 4 is that the time window where coherent cooperation is possible depends on the position of the UE. Since all cooperation areas include the region surrounding the center of the beam, those users located close to the beam center will benefit from dual satellite transmission for a longer period than those users located close to the beam edge. This is clearly evidenced from the shape of the cooperation area at $t-30$ seconds and at $t+30$ seconds. In this respect, at Position 3, the UE could enjoy joint satellite transmission for at least 1 minute. The rest of the simulation results will be shown considering a UE that is located at Position 1. This is the most challenging situation, because the UE is close to the edge of the beam. At the time instant t, we found that the normalized time and frequency offsets are $(i_{\text{eff}}, q_{\text{eff}}, \kappa_{\text{eff}}) = (504, -2, 0.236)$.

To compute the spectral efficiency, we consider the system model formulated in (23), as detailed in [13]. In Figure 5, we compare single and dual satellite operation in terms of spectral efficiency versus N_R. When $8^2 \leq N_R \leq 24^2$, the received SNR, which is defined as $SNR_k = \frac{EIRP \cdot N_R}{L_k B_W K_B T}$, ranges from 5.41 (4.43) dB to 14.95 (13.97) dB for $k=1$ ($k=2$). We have considered that the symbols are drawn from 16QAM and QPSK constellations. As expected, the highest spectral efficiency is provided by OTFS dual, because the two satellite links with similar channel gain are added coherently. The improvement comes from the increased energy that is received. Accordingly, the adoption of OTFS dual significantly reduces the number of receive antennas required to reach a target spectrum efficiency.

If we drive the attention to the reliability, we observe in Figure 6 that the possibility of having two satellite links can be harnessed in conjunction with OTFS to reduce the uncoded bit error rate (BER). OTFS dual clearly outperforms OFDM single, because the receiver is able to add coherently two satellite signals of similar strength. The results also reveal that the residual interference in OTFS is negligible. Otherwise, any error floor would manifest in the target SNR range.

VI. Conclusions

This paper proposes an OTFS-based dual satellite joint transmission scheme. The system is conceived to achieve perfect synchronization in a selected reference point. Under this premise, we have analytically characterized the cooperation area where satellite signals can be combined coherently. The key is to precode the symbols in the delay-Doppler domain to effectively counteract residual time and frequency offsets resulting from the displacement of the receiver from the selected reference point. The attention has been focused on dual satellite transmission. Simulation results show that significant improvements in terms of spectrum efficiency as well as uncoded BER are achieved with respect to OFDM-based single satellite systems. Practical implementation aspects and the consideration of the receiver mobility will be investigated in future works.

References

[1] "3GPP; Technical Specification Group Radio Access Network; Multi-connectivity Stage 2 (Release 16)." 3GPP TS 37.340.

[2] Röper et al., "Robust distributed MMSE precoding in satellite constellations for downlink transmission," in *2019 IEEE 2nd 5G World Forum (5GWF)*, 2019, pp. 642–647.

[3] Guidotti et al., "Beamforming in LEO Constellations for NB-IoT Services in 6G Communications," *CoRR*, vol. abs/2103.13348, 2021.

[4] Röper et al., "Beamspace MIMO for Satellite Swarms," in *IEEE WCNC (to appear), Austin, TX, USA*, 2022.

[5] Raviteja et al., "Practical Pulse-Shaping Waveforms for Reduced-Cyclic-Prefix OTFS," *IEEE Trans. Veh. Technol.*, vol. 68, no. 1, pp. 957–961, 2019.

[6] T. Li et al., "OTFS modulation performance in a satellite-to-ground channel at sub-6-GHz and millimeter-wave bands with high mobility," *Front. Inf. Technol. Electron. Eng.*, vol. 22, no. 4, pp. 517–526, 2021.

[7] Amit Sravan Bora et al., "Spatially Correlated MIMO-OTFS for LEO Satellite Communication Systems," in *ICC Workshops*, 2022.

[8] Zhang et al., "Hybrid Beamforming for 5G and Beyond Millimeter-Wave Systems: A Holistic View," *IEEE Open J. Commun. Soc.*, vol. 1, pp. 77–91, 2020.

[9] B.C. Pandey et al., "Low Complexity Precoding and Detection in Multi-User Massive MIMO OTFS Downlink," *IEEE Veh. Technol. Mag.*, vol. 70, no. 5, pp. 4389–4405, 2021.

[10] Pachler et al., "An Updated Comparison of Four Low Earth Orbit Satellite Constellation Systems to Provide Global Broadband," in *IEEE ICC Workshops*, 2021, pp. 1–7.

[11] Osoro et al., "A Techno-Economic Framework for Satellite Networks Applied to Low Earth Orbit Constellations: Assessing Starlink, OneWeb and Kuiper," *IEEE Access*, vol. 9, pp. 141 611–141 625, 2021.

[12] "3GPP; Technical Specification Group Radio Access Network; NR; Physical channels and modulation; (Release 16)." 3GPP TS 38.211.

[13] Caire et al., "Bit-interleaved coded modulation," *IEEE Trans. Inf. Theory*, vol. 44, no. 3, pp. 927–946, 1998.